

The Society shall not be responsible for statements or opinions advanced in papers or in discussion at meetings of the Society or of its Divisions or Sections, or printed in its publications Discussion is printed only if the paper is published in an ASME Journal Papers are available from ASME for fifteen months after the meeting.

Printed in USA

Dynamic Stress on a Partially Bonded Fiber

Andrew Norris

Assoc. Mem. ASME

Yang Yang

Department of Mechanics and Materials Science, Rutgers University, Piscataway, NJ 08855-0909 The dynamic stress on a partially bonded fiber is analyzed for shear wave incidence, with particular attention given to the stress intensity factor at the neck joining the fiber to the matrix. The problem is formulated in terms of the unknown stress across the neck and the remainder of the fiber-matrix interface is modeled as a curved interfacial crack. Explicit asymptotic expressions are derived for the near and farfields that are valid in the frequency range in which the recently discussed resonance phenomenon occurs (Yang and Norris, 1991). This resonance is a rattling effect that is most prominent when the neck becomes very thin, and can occur at arbitrarily small values of the dimensionless frequency ka, where a is the radius of the fiber. The asymptotic results indicate that the dynamic stress intensity factor becomes unbounded as the neck vanishes, in contrast to the prediction of a purely quasistatic analysis that the stress intensity factor vanishes in the same limit.

1 Introduction

In a recent analysis of the scattering of out-of-plane shear waves from a partially debonded fiber in an otherwise homogeneous matrix, it was demonstrated that the fiber can exhibit a strong resonance at very low frequencies (Yang and Norris, 1991). The reason for this is apparent from Fig. 1: As the size of the debond becomes large, the neck joining the fiber to the matrix becomes correspondingly smaller, allowing the fiber to undergo large relative motion. At the same time the mass of the fiber is unchanged, and thus the fiber acts as a spring-mass system of constant mass and relatively small stiffness. The stiffness goes to zero as the neck vanishes, and so one expects that the frequency of resonance also goes to zero in the same limit. The numerical results of Yang and Norris (1991) clearly show that the resonance can be excited by incident shear waves, and that it can occur at arbitrarily low frequency if the neck is allowed to be sufficiently small.

This type of resonance is clearly related to the Helmholtz resonance of gravity water waves in a harbor with a narrow opening (Miles, 1971; Burrows, 1985), and more generally, with the Helmholtz resonance phenomenon of an acoustical cavity. In the latter case, the compressibility of the acoustic fluid occupying the cavity is volumetric, but the mass of entrained fluid in the cavity opening is independent of the cavity volume, depending instead on the local geometry at the mouth. Thus, the roles of stiffness and inertia are quite different in the fiber and Helmholtz resonances.

Contributed by the Applied Mechanics Division of THE AMERICAN SOCIETY OF MECHANICAL ENGINEERS for presentation at the Joint Applied Mechanics/Bioengineering Conference, Ohio State University, Columbus, Ohio, June 16-19, 1991.

Discussion on this paper should be addressed to the Technical Editor, Prof. Leon M. Keer, the Technological Institute, Northwestern University, Evanston, IL 60208, and will be accepted until two months after final publication of the paper itself in the JOURNAL OF APPLIED MECHANICS. Manuscript received by the ASME Applied Mechanics Division, Mar. 20,1990; final revision, July 30, 1990. Paper No. 91-APM-30.

Copies of this paper will be available until Sept. 1992.

One consequence of the fiber resonance is that the scattering cross-section of a low frequency shear wave is greatly enhanced, thus providing a possible means of identifying loose fibers using ultrasonic waves. The numerical results of Yang and Norris (1991) also show that the stress intensity factor at the neck is magnified at resonance, which has important implications for the dynamic pullout of fibers and shock-induced debonding and may also be of significance in the vibration of foundation pilings subject to seismic excitation. These increases in response at resonance are analogous to the paradoxical enhancement of the surge in a harbor as the entrance

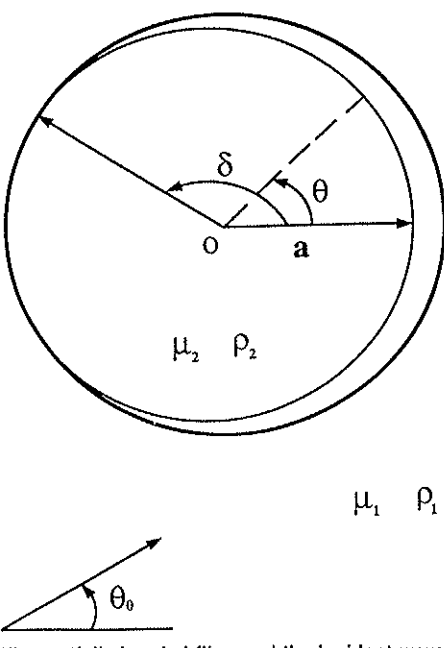


Fig. 1 The partially bonded fiber and the incident wave direction

is narrowed, an effect known as the "harbor paradox" (Miles, 1971; Burrows, 1985). In the present paper we focus on the dynamic stress intensity factor using a formulation which leads directly to simple asymptotic expressions for the resonance frequency and the stress intensity factor for small neck size. In the previous analysis (Yang and Norris, 1991) a system of equations was derived for the coefficients in a Chebyshev expansion of the crack opening displacement of the debond. This is the standard approach in attacking scattering problems involving cracks in infinite media (Krenk and Schmidt, 1982; Boström, 1987), and leads to simplifications in the present configuration when the debond is small, but is not suitable for treating the limit in which the neck as very narrow. In this paper we consider the stress on the neck is the unknown to be determined, rather than the COD. This method is similar in spirit to that of Burrows (1985) who considered waves incident on a circular harbor, and some of the asymptotic results reported here are similar to his discussions of the "harbor paradox." One advantage of the present method of solution is that the unperturbed configuration is the fully debonded state (i.e., a void) whereas in the COD method the base state is the perfectly bonded fiber. The dynamic response is simpler for the void and although this simplification is not significant for the SH problem treated here, it is very useful in considering the in-plane problem, the results of which will be published separately.

The formulation and analysis are developed in Sections 2, 3, and 4, and the main discussion regarding the stress intensity factor is in Section 5. Numerical calculations are presented in Section 6.

2 Formulation

The fiber occupies the region r < a (see Fig. 1) with density ρ_2 and shear modulus μ_2 , and the matrix r > a has corresponding parameters ρ_1 and μ_1 . The motion is out of the plane with time harmonic dependence $\exp(-i\omega t)$ which is omitted in all equations. The debond is of angular width 2δ , or equivalently, the extent of the neck is 2ϵ , where $\epsilon = \pi - \delta$. The total out-of-plane displacement is

$$u^{\text{tot}} = \begin{cases} u^{in} + u_1^{(0)} + u_1^{(1)}, & r > a, \\ u_2^{(1)}, & r < a, \end{cases}$$
 (1)

where u^{in} is the incident wave and $u_1^{(0)}$ is the scattered field from the void r < a, which satisfies the boundary condition

$$\mu_1 \left(\frac{\partial u^{in}}{\partial r} + \frac{\partial u_1^{(0)}}{\partial r} \right) = 0, \quad r = a, \quad -\pi < \theta < \pi,$$
(2)

with the appropriate radiation condition at infinity. The total stress must be continuous over the entire interface, implying

$$\mu_1 \frac{\partial u_1^{(1)}}{\partial r} = \mu_2 \frac{\partial u_2^{(1)}}{\partial r} = \begin{cases} 0, & r = a, & -\delta < \theta < \delta, \\ \tau(\theta), & r = a, & \delta < |\theta| < \pi \end{cases}$$
(3)

where $\tau(\theta)$ is the unknown additional stress on the neck.

The displacement continuity condition on the neck $\delta < |\theta| < \pi$ is

$$u^{in} + u_1^{(0)} + u_1^{(1)} = u_2^{(1)}, \quad r = a, \quad \delta < |\theta| < \pi.$$
 (4)

The incident field is assumed to be a plane wave of amplitude A

$$u^{in} = Ae^{ik_1r\cos(\theta - \theta_0)} = A\sum_{n=0}^{\infty} \epsilon_n i^n J_n(k_1r)\cos n(\theta - \theta_0), \quad (5)$$

where $\epsilon_0 = 1$, $\epsilon_n = 2$, n > 0, and $k_i = \omega/c_i$, $c_i = [\mu_i/\rho_i]^{1/2}$, i = 1, 2. The scattered field from the void is then

$$u_1^{(0)} = -A \sum_{n=0}^{\infty} \frac{\epsilon_n i^n J_n'(k_1 a)}{H_n^{(1)}(k_1 a)} H_n^{(1)}(k_1 r) \cos n(\theta - \theta_0).$$
 (6)

Finally, the additional fields $u_1^{(1)}$ and $u_2^{(1)}$ must satisfy the Helmholtz equations

$$\nabla^2 u_i^{(1)} + k_i^2 u_i^{(1)} = 0, \quad i = 1 \text{ or } 2,$$
 (7)

in the respective regions, where ∇^2 is the 2D Laplacian.

3 The Symmetric Solution

The total field may be separated into parts that are either symmetric or antisymmetric about $\theta = 0$. We concern ourselves here only with the symmetric part since the treatment of the antisymmetric part is very similar (Yang and Norris, 1991). The symmetric part of the additional fields may be expressed, using equation (3), as

$$u_{1s}^{(1)} = \sum_{n=0}^{\infty} E_n^{(s)} H_n^{(1)}(k_1 r) \cos n\theta,$$

$$u_{2s}^{(1)} = \sum_{r=0}^{\infty} \frac{\mu_1 k_1 E_n^{(s)} H_n^{(1)}(k_1 a)}{\mu_2 k_2 J_n'(k_2 a)} J_n(k_2 r) \cos n\theta. \quad (8)$$

Use of (3), (8), and the orthogonality of the cosine functions gives

$$E_n^{(s)} = \frac{\epsilon_n}{\pi \mu_1 k_1 H_n^{(1)} (k_1 a)} \int_{\delta}^{\pi} \tau(\theta) \cos n\theta \ d\theta. \tag{9}$$

Substitution of (5), (6), (8), and (9) into (4), and use of the Wronskian relations (Abramowitz and Stegun, 1965), yields an integral equation for the stress

$$2iA \frac{\mu_2 k_2}{k_1 a} \sum_{n=0}^{\infty} \frac{\epsilon_n t^n \cos n\theta_0}{H_n^{(1)'}(k_1 a)} \cos n\theta$$

$$= \sum_{n=0}^{\infty} \epsilon_n \Lambda_n \cos n\theta \int_{\delta}^{\infty} \tau(\theta') \cos n\theta' d\theta', \quad (10)$$

where

$$\Lambda_n = \frac{J_n(k_2 a)}{J_n'(k_2 a)} - \frac{\mu_2 k_2}{\mu_1 k_1} \frac{H_n^{(1)}(k_1 a)}{H_n^{(1)}(k_1 a)}.$$
 (11)

The unknown shear stress $\tau(\theta)$ can be expressed using the first kind of Chebyshev polynomials

$$\tau(\theta) = \frac{Ai\mu_1 k_1}{\sqrt{1 - \left(\frac{\pi - \theta}{\epsilon}\right)^2}} \sum_{n=0}^{\infty} \beta_n^{(s)} \phi_n^{(s)}(\theta), \tag{12}$$

where (Abramowitz and Stegun, 1965)

$$\phi_n^{(s)}(\theta) = (-1)^n T_{2n} \left(\frac{\pi - \theta}{\epsilon} \right)$$

$$= (-1)^n \cos \left(2n \arccos \frac{\pi - \theta}{\epsilon} \right). \quad (13)$$

Note that $\tau(\theta)$ has the correct inverse square root singularity at either end of the neck. The Chebyshev functions have the property

$$\int_{\delta}^{\pi} \frac{\phi_n^{(s)}(\theta)}{\sqrt{1 - \left(\frac{\pi - \theta}{\epsilon}\right)^2}} \cos p\theta \ d\theta = (-1)^p \frac{\pi \epsilon}{2} J_{2n}(p\epsilon), \quad (14)$$

and it is therefore possible to reduce (10) to a system of equations for the coefficients $\beta_n^{(s)}$

$$\sum_{n=0}^{\infty} Q_{mn}^{(s)} \beta_n^{(s)} = N_m^{(s)}, \quad m = 0, 1, 2, \dots,$$
 (15)

where

$$Q_{mn}^{(s)} = \frac{1}{2} \sum_{p=0}^{\infty} \epsilon_p \Lambda_p J_{2m}(p\epsilon) J_{2n}(p\epsilon),$$

$$N_m^{(s)} = \frac{2}{\pi \epsilon k_1 a} \frac{\mu_2 k_2}{\mu_1 k_1} \sum_{p=0}^{\infty} \epsilon_p \frac{(-i)^p J_{2m}(p\epsilon)}{H_p^{(1)}'(k_1 a)} \cos p\theta_0. \quad (16)$$

In practice, the system of equations (15) is solved by truncation. Also, as we will see below, the term $Q_0^{(s)}$ is singular at low frequencies. In order to avoid an ill-conditioned system in the static limit, we eliminate $\beta_0^{(s)}$ using the equation for m=0, and then solve the resulting system.

4 The Scattered Radiation Pattern

The scattered symmetric displacement due to the debond follows from (8), (9), (12), and (14), and the far-field approximation for $u_{1s}^{(1)}$ becomes

$$u_{1s}^{(1)} \sim \left(\frac{8\pi}{k_1 r}\right)^{1/2} F_s^{(1)}(\theta, \theta_0) e^{i\left(k_1 r - \frac{\pi}{4}\right)}, \quad k_1 r \to \infty,$$
 (17)

where the radiation pattern generated by the debond is

$$F_s^{(1)}(\theta,\theta_0) = \frac{Ai\epsilon}{4\pi} \left(\frac{\beta_0^{(s)}}{H_0^{(1)'}(k_1 a)} + 2 \sum_{p=1}^{\infty} \frac{f^p \cos p\theta}{H_p^{(1)'}(k_1 a)} \sum_{n=1}^{\infty} \beta_n^{(s)} J_{2n}(p\epsilon) \right). \quad (18)$$

At low frequencies such that $k_1a \ll 1$, $k_2a \ll 1$, but for fixed $\epsilon = O(1)$, it may be shown that $\beta_0^{(s)} = O(k_2a)$, and therefore $\beta_0^{(s)} \to 0$ as $k_1a \to 0$ in agreement with the static condition that the net force acting on the fiber is zero. The net moment on the fiber is automatically zero for the symmetric solution and may be shown to be $O(k_1a)$ for the antisymmetric solution. The symmetric far-field becomes, in this limit,

$$F_s^{(1)}(\theta,\theta_0) = \frac{Ai}{4} (k_1 a)^2 \left(\frac{\rho_2}{2\rho_1} + \epsilon \cos \theta \sum_{n=1}^{\infty} \tilde{\beta}_n^{(s)} J_{2n}(\epsilon)\right) + o(k_1 a)^2.$$
 (19)

where the $\tilde{\beta}_{n}^{(s)}$ are real valued and satisfy

$$\sum_{n=1}^{\infty} \tilde{Q}_{mn}^{(s)} \tilde{\beta}_{n}^{(s)} = \frac{-2\mu_{2}}{\epsilon(\mu_{1} + \mu_{2})} \cos \theta_{0} J_{2m}(\epsilon), \quad m = 1, 2, \dots, \quad (20)$$

and

$$\tilde{Q}_{nm}^{(s)} = \sum_{p=1}^{\infty} \frac{1}{p} J_{2m}(p\epsilon) J_{2n}(p\epsilon). \tag{21}$$

It should be noted that the monopole term in (19), i.e., the term involving the densities, comes from the low frequency limit of $\beta_0^{(s)}$, which is discussed in the next section.

A system of equations very similar to (20) was encountered in the COD formulation of Yang and Norris (1991) for the same problem, but in that case the matrix \tilde{Q} and the right-hand side of the system both depended upon $\delta = \pi - \epsilon$ rather than ϵ . Furthermore, the system corresponding to (20) was previously obtained for the antisymmetric part of the solution. However, based on the analogy with the equations in Yang and Norris (1991) it can be shown that the sum in equation (19) may be simplified, and a similar result is found for the antisymmetric far-field pattern $F_a^{(1)}(\theta, \theta_0)$. Combining these results we find that the total radiation pattern in the low frequency limit is in complete agreement with the quasi-static far-field obtained by Coussy (1982) using the purely static solution discussed below.

5 Stress Intensity Factors and Resonance

The dynamic stress intensity factor at the junction of the neck and debond is defined as

$$KI_d = \lim_{\theta \to \lambda^+} \left[2a(\theta - \delta) \right]^{\frac{1}{2}} \tau(\theta), \tag{22}$$

and so it follows from (12) and (13) that

$$\frac{KI_d^{(s)}}{\tau_0\sqrt{a}} = \sqrt{\epsilon} \sum_{n=1}^{\infty} (-1)^n \beta_n^{(s)}, \tag{23}$$

where $\tau_0 = i\mu_1 k_1 A$ is the stress applied at infinity in the static limit, and in general, $\beta_n^{(s)}$ are frequency dependent and determined from (15). The shear stress $\tau_s(\theta)$ along the bonded interface for the corresponding static problem may be expressed in closed form using the solution obtained by Tamate and Yamada (1969).

$$\tau_{s}(\theta) = \frac{\tau_{0}\mu_{2}}{\mu_{1} + \mu_{2}} \frac{\sin\left(\frac{3\theta}{2} - \theta_{0}\right) - \cos\delta\sin\left(\frac{\theta}{2} - \theta_{0}\right)}{\sqrt{\sin\frac{\theta + \delta}{2}\sin\frac{\theta + \delta}{2}}} \operatorname{sgn}(\theta),$$

$$\delta < |\theta| < \pi. \quad (24)$$

The static SIF follows from equation (22) as $KI_s = KI_s^{(a)} + KI_s^{(a)}$, with symmetric and antisymmetric parts

$$\frac{KI_s^{(s)}}{\tau_0\sqrt{a}} = \frac{2\mu_2}{\mu_2 + \mu_2} \sqrt{\sin\epsilon} \sin\frac{\epsilon}{2}\cos\theta_0,$$

$$\frac{KI_s^{(a)}}{\tau_0\sqrt{a}} = \frac{2\mu_2}{\mu_1 + \mu_2} \sqrt{\sin\epsilon} \cos\frac{\epsilon}{2}\sin\theta_0. \quad (25)$$

We note in particular that for fixed θ_0 , $KI_s^{(s)} = O(\epsilon^{3/2})$ and $KI_s^{(a)} = O(\epsilon^{1/2})$ as $\epsilon \to 0$.

5.1 The Short Neck Approximation. As the fiber becomes almost separated from the matrix ($\epsilon \ll 1$), equation (15) can be simplified quite a bit. Considering m or n > 0,

$$Q_{mn}^{(s)} = \sum_{p=1}^{\left[\frac{1}{\sqrt{\epsilon}}\right]-1} \Lambda_p J_{2m}(p\epsilon) J_{2n}(p\epsilon) + \sum_{p=1}^{\infty} \Lambda_p J_{2m}(p\epsilon) J_{2n}(p\epsilon), \quad (26)$$

$$\left[\frac{1}{\sqrt{\epsilon}}\right]$$

where $\left[\frac{1}{\sqrt{\epsilon}}\right]$ is the integer part of $\frac{1}{\sqrt{\epsilon}}$. The first sum is $O(\epsilon^{m+n})$,

while the infinite sum simplifies by using asymptotic expansion for large order Bessel and Hankel functions, to give

$$\sum_{n=0}^{\infty} \Lambda_p J_{2m}(p\epsilon) J_{2n}(p\epsilon)$$

$$= k_2 a \left(1 + \frac{\mu_2}{\mu_1} \right) \int_0^{\infty} \frac{J_{2m}(\nu) J_{2n}(\nu)}{\nu} d\nu + O(\epsilon),$$

and the integral may be found in Abramowitz and Stegun (1965). In summary, we have the asymptotic results for $\epsilon \ll 1$ that

$$Q_{mn}^{(s)} = k_2 a \left(1 + \frac{\mu_2}{\mu_1} \right) \frac{\delta_{mn}}{4m} + O(\epsilon),$$

$$N_m^{(s)} = O(\epsilon^{2m-1}), \quad m > 0, \quad (27)$$

and from (15) and (27),

$$\beta_0^{(s)} = \frac{N_0^{(s)}}{Q_0^{(s)}} + O(\epsilon), \quad \beta_m^{(s)} = O(\epsilon^{2m-1}), \quad m > 0.$$
 (28)

Equation (28) indicates that the response of the fiber when the neck is small is governed principally by the first term in the expansion (12) for the stress $\tau(\theta)$. Since the first Chebyshev function $\phi_0^{(s)}$ is unity, it follows that the approximate stress in this regime is

 $\tau(\theta) = \frac{\tau_0 \beta_0^{(s)}}{\sqrt{1 - \left(\frac{\pi - \theta}{\epsilon}\right)^2}}.$ (29)

The relatively simple form of $\beta_0^{(s)}$ in (28) means that the resonance reported by Yang and Norris (1991) and illustrated in the numerical examples below is governed by this expression only, rather than the full system of equations (15). It is also clear, if not a priori then certainly a posteriori, that the resonance must occur at asymptotically small values of k_1a . Therefore, in order to further understand the resonance, we further approximate $\beta_0^{(s)}$ as a doubly asymptotic expansion in both ϵ and k_1a . Expansion of the numerator and denominator in (28) for low frequencies yields

$$\beta_0^{(s)} \sim \frac{ik_2 a}{\epsilon} \frac{\mu_2 k_2}{\mu_1 k_1} f(k_1 a, \epsilon, \theta_0), \tag{30}$$

where

 $f(k_1a,\epsilon,\theta_0)$

$$= \frac{1 - 2ik_1a\cos\theta_0}{1 - \frac{\mu_2}{\mu_1}(k_2a)^2 \left[\left(1 + \frac{\mu_1}{\mu_2}\right)S(\epsilon) + \frac{\mu_1}{8\mu_2} - \frac{\gamma}{2} - \frac{1}{2}\log\frac{k_1a}{2} + i\frac{\pi}{4}\right]},$$
(31)

$$S(\epsilon) = \sum_{p=1}^{\infty} \frac{J_0^2(p\epsilon)}{p},$$
 (32)

and γ is Euler's constant. We note that f is asymptotic to unity for $\epsilon = O(1)$, in which case (30) reproduces the low-frequency behavior of $\beta_0^{(s)}$ discussed in Section 4. However, in the doubly asymptotic regime of $\epsilon \ll 1$, $k_1 a \ll 1$, f depends upon ϵ through $S(\epsilon)$ which can be simplified by first using the identity $J_0(x) = \pi^{-1} \int_0^{\pi} \cos(x \sin t) dt$. The sum over p then follows from equation (27.8.6) of Abramowitz and Stegun (1965) to give

$$S(\epsilon) = \frac{-1}{2\pi^2} \int_0^{\pi} \int_0^{\pi} \left\{ \log \left[2 \sin \frac{\epsilon}{2} |\sin t - \sin s| \right] + \log \left[2 \sin \frac{\epsilon}{2} (\sin t + \sin s) \right] \right\} ds dt.$$

Expanding the integrand in ϵ and using equation (4.226.1) of Gradshteyn and Ryzhik (1980) yields

$$S(\epsilon) = \log\left(\frac{2}{\epsilon}\right) + \frac{\epsilon^2}{6} + O(\epsilon^4). \tag{33}$$

The term $S(\epsilon)$ is asymptotically large and therefore f may vary considerably from unity even as the frequency goes to zero, in stark contrast to the quasi-static behavior based on the static solution.

This low-frequency effect is manifested as the resonance discussed in the Introduction. To a first approximation, the resonance occurs when the real part of the denominator in (31) vanishes, i.e., at frequency k_1a which satisfies

$$\left(1 + \frac{\mu_2}{\mu_1}\right) \log \frac{2}{\epsilon} = \frac{1}{(k_2 a)^2} - \frac{1}{8} + \frac{\mu_2}{2\mu_1} \left[\gamma + \log \left(\frac{k_1 a}{2}\right) \right]. \quad (34)$$

This reduces to equation (20) of Burrows (1985) when the material parameters are equal on either side of the neck ($\mu_1 = \mu_2$, $\rho_1 = \rho_2$). The leading-order approximation for $\epsilon \ll 1$ is

$$k_2 a = \beta^{-1} \left[\log \left(\frac{2}{\epsilon} \right) \right]^{-\frac{1}{2}}, \quad \beta = \sqrt{1 + \frac{\mu_2}{\mu_1}},$$
 (35)

and so the resonant frequency thus goes to zero very slowly as $\epsilon \rightarrow 0$. Yang and Norris (1991) proposed a heuristic springmass model of the low-frequency resonance which predicted the resonant frequency in the same form as (35), but the simplicity of the model did not permit the explicit evaluation of β in (35), which was originally cast as an unknown constant. However, it is clear that the model does give the correct leadingorder behavior. Furthermore, the precise form of β means that the resonant frequency can be simply modeled as the frequency of a spring-mass system with mass $m = 2\rho_2\pi a^2$, which is twice the mass of a unit length of the fiber. This is not surprising when one considers that as the fiber oscillates, an equivalent inertial mass of matrix oscillates out of phase. The effective stiffness K of the oscillator follows from Yang and Norris (1991) as the ratio F/w, where F is a uniformly applied axial force over an isolated fiber of shear modulus equal to the harmonic mean of the matrix and fiber moduli, i.e., μ^{-1} $\frac{1}{2}(\mu_1^{-1} + \mu_2^{-1})$. An equal but opposite force is distributed across the portion of the boundary corresponding to the neck such that the applied shear has the correct inverse square root singularity, and w is the resultant average static displacement of the fiber in the direction of the axial force. The resonant frequency predicted by this model is the frequency of equation (35). It is interesting to note that simple, equivalent-circuit models for the harbor resonance phenomenon have been proposed and discussed at length by Miles (1971). The present phenomenon is, however, probably better understood in terms of mechanical lumped-parameter models.

6 Numerical Results and Discussion

The stress and stress intensity factor have been computed for the matrix/fiber combination of epoxy and glass: $\mu_1 = 1.28$ GPa, $\rho_1 = 1.25$ gm/cc, and $\mu_2 = 29.9$ GPa, $\rho_2 = 2.55$ gm/cc. The calculations were performed by truncating the infinite system of equations (15), and were checked by (i) requiring that the optical theorem was satisfied to a given degree of tolerance, and (ii) by comparing the results with those obtained using the COD method of Yang and Norris (1991). The latter method was found to be numerically fast for small crack sizes, but required larger and larger truncation limits as δ approached 180 deg. For reasons mentioned previously, the system (15) is in a sense the dual of that obtained by Yang and Norris (1991), and not surprisingly, we found the system required only a small truncation limit for small necks but became unwieldy for small cracks.

The ratio of the dynamic stress intensity factor to the static SIF is plotted in Figs. 2 and 3 for different neck widths. The corresponding quasi-static theory would predict a constant SIF at such low frequencies as those considered in the figures, and normally one would not expect any appreciable change until the dimensionless frequency k_1a is of order unity. However, the dynamic SIFs in Figs. 2 and 3 clearly exhibit a resonance behavior at a frequency that decreases with ϵ . Note in particular the enormous magnification of the dynamic SIF at resonance, as compared with the static prediction.

The predictions based upon the doubly asymptotic theory of Section 5 are compared with the exact computations in Figs. 4 and 5. It should be noted that the asymptotic theory contains no free parameters. The agreement between the full, numerically intensive computations, and the simple asymptotic theory is excellent, and appears to be reasonable even when both ϵ and k_1a are of order unity. In fact, the leading-order approximation of equation (35) turns out to be a very good indicator of the resonance frequency. We note that the magnitude of the dynamic SIF becomes unbounded as the neck width vanishes, in stark contrast to the static prediction that the static SIF goes to zero as $\epsilon^{1/2}$ if the applied stress has an antisymmetric

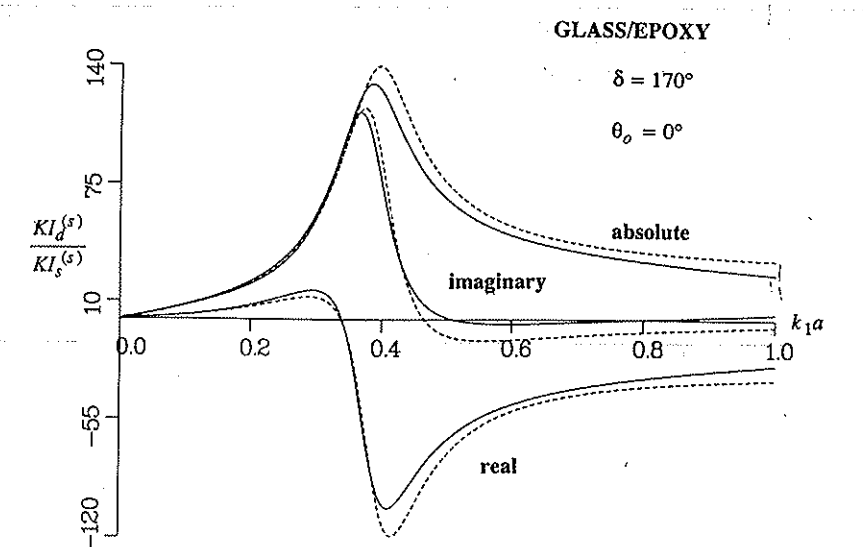


Fig. 2 The complex-valued ratio of the dynamic stress intensity factor to the static SIF versus nondimensional frequency k_1a for glass/epoxy, $\delta=170$ deg ($\epsilon=10$ deg) and $\theta_0=0$. The solid curves are the results of the "exact" numerical calculations, and the dashed curves follow from the asymptotic approximation of equation (37).

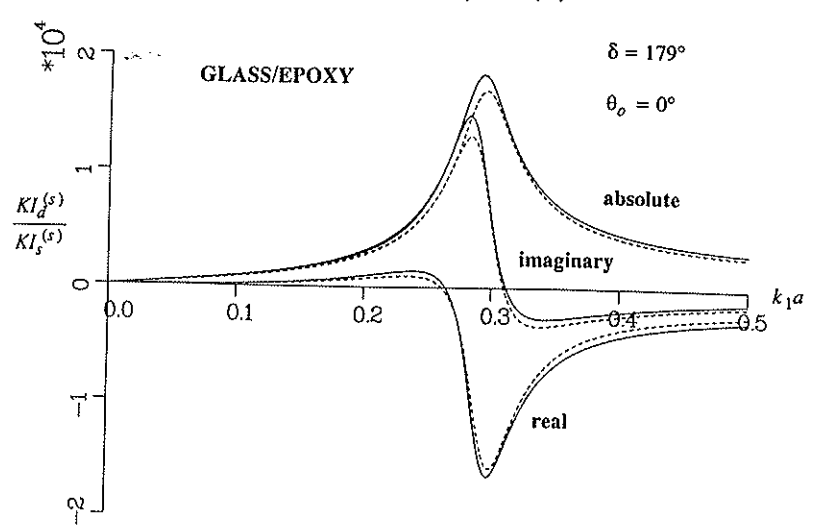


Fig. 3 The same as Fig. 2, but for $\delta = 179 \deg (\epsilon = 1 \deg)$

component and as $\epsilon^{3/2}$ if not. Also, the real part of the SIF at resonance achieves a large but negative value, i.e. it is 180 deg out of phase with the static SIF.

The accuracy of the asymptotic approximation supports the conclusion that stress field $\tau(\theta)$ on the neck is governed mainly by the first term in the expansion (12) when $\epsilon \ll 1$ and $k_1 a \ll 1$. For fixed ϵ but $k_1 a \ll 0$, the exact theory reproduces the static stress $\tau_s(\theta)$ of equation (24), and as discussed in Section 4, the term $\beta_0^{(s)} \to 0$, while the remaining $\beta_n^{(s)}$, $n \geq 1$, are of order unity. Therefore, the purely static and the doubly asymptotic limits are in a sense complementary, and we are justified in combining both to form a new approximation uniformly valid in both asymptotic regimes. We call this the quasidynamic approximation, since it goes beyond the quasi-static approximation based on the static solution, but is not a fully dynamic solution. When the relevant terms are combined, we obtain for the quasi-dynamic stress

$$\tau_{qd}(\theta) = \tau_s(\theta) + \frac{\tau_0 i k_2 a}{\sqrt{\epsilon^2 - (\pi - \theta)^2}} \frac{\mu_2 k_2}{\mu_1 k_1} f(k_1 a, \epsilon, \theta_0), \quad (36)$$

where f is defined in (31) and (33). The quasi-dynamic stress intensity factor KI_{ad} is thus

$$KI_{qd} = KI_s + \tau_0 i k_2 a \left(\frac{a}{\epsilon}\right)^{1/2} \frac{\mu_2 k_2}{\mu_1 k_1} f(k_1 a, \epsilon, \theta_0). \tag{37}$$

These expressions are uniformly valid for both small ϵ and k_1a , and obviously contain the resonance features of Figs. 2-5. The associated scattered field may be easily computed and it turns out that the far-field pattern is changed only in the monopole term.

In conclusion, we have obtained simple but accurate expressions that fully describe the low-frequency resonant behavior. The numerical and analytical results demonstrate that the stress intensity factor at the neck of the fiber can be greatly magnified in comparison with the static prediction. Thus, for instance, failure predictions based solely upon a static analysis could be quite erroneous.

Acknowledgment

We are grateful to a reviewer for the asymptotic approximation of equation (33).

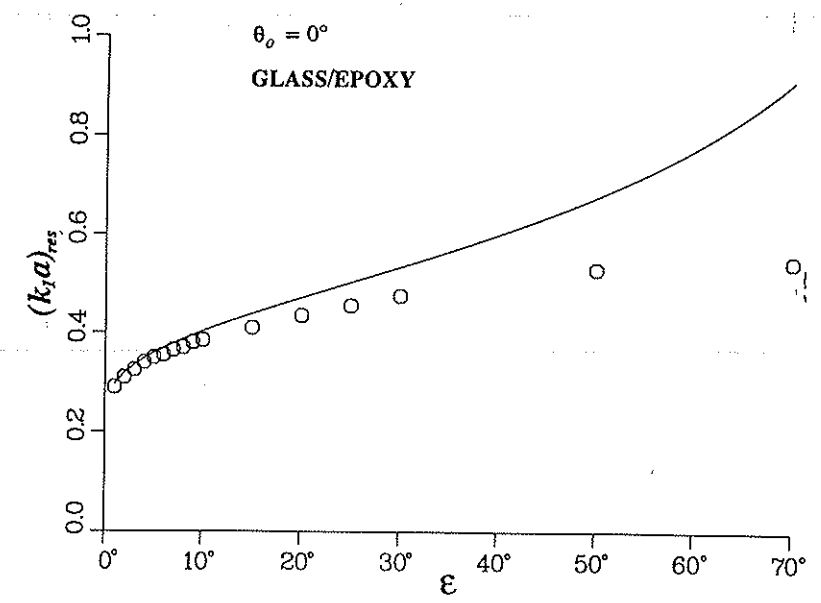


Fig. 4 The dimensionless resonant frequency according to the approximate theory, equation (34), compared with the frequency at which the magnitude of the dynamic SIF achieves a maximum in the exact calculations

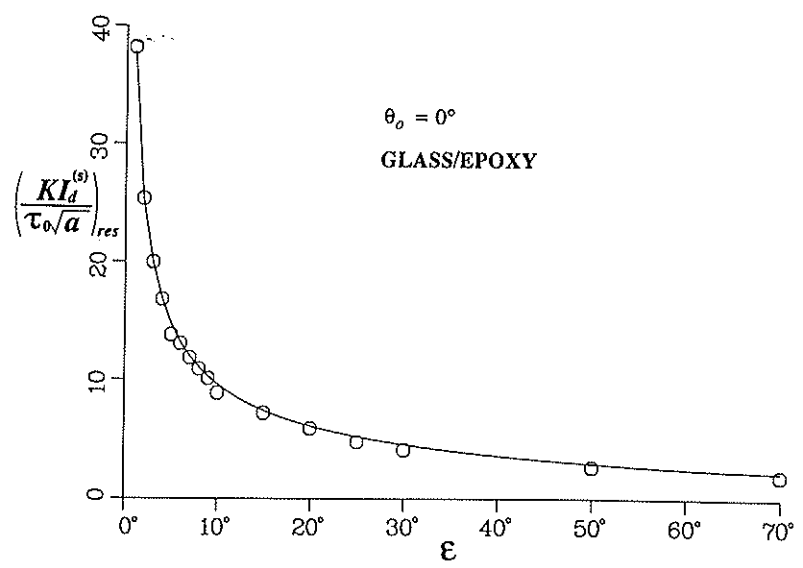


Fig. 5 A comparison of the magnitude of the dimensionless dynamic stress intensity factor at resonance versus the neck angular width ϵ . The solid curve is calculated using the asymptotic expansion of the stress on the neck, equations (12) and (30)-(34). The circles are the numerical computations of the exact solution, equation (15).

References

Abramowitz, M., and Stegun, I. A., 1965, Handbook of Mathematical Functions, Dover Publications, New York.

Boström, A., 1987, "Elastic Wave Scattering from an Interface Crack: Antiplane Strain," ASME JOURNAL OF APPLIED MECHANICS, Vol. 55, pp. 503-508.

Burrows, A., 1985, "Waves Incident on a Circular Harbour," Proceeding of

the Royal Society of London, Vol. A401, pp. 349-371.

Coussy, O., 1982, "Scattering of SH-Waves by a Cylindrical Inclusion Presenting an Interfacial Crack," C. R. Acad Sc. Paris, Vol. 295, pp. 1043-1046.

Gradshteyn, I. S., and Ryzhik, I. B., 1980, Tables of Integrals, Series, and Products, Academic Press, New York.

Krenk, S., and Schmidt, H., 1982, "Elastic Wave Scattering by a Circular

Crack," Philosophical Transactions of the Royal Society of London, Vol. A308, pp. 167-198.

Miles, J. W., 1971, "Resonant Response of Harbors: An Equivalent-Circuit Analysis," Journal of Fluid Mechanics, Vol. 46, pp. 241-265.

Tamate, O., and Yamada, T., 1969, "Stress in an Infinite Body with a Partially

Bonded Circular Cylindrical Inclusion under Longitudinal Shear," Technology Reports, Tohoku University, Vol. 34, pp. 161-171.
Yang, Y., and Norris, A. N., 1991, "Shear Wave Scattering from a Debonded

Fibre," Journal of the Mechanics and Physics of Solids, Vol. 39, pp. 273-294.